Classification of Energy Levels in Al^{25}*

LOUIS J. KOESTER, JR.†
University of Wisconsin, Madison, Wisconsin
(Received October 1, 1951)

The differential cross section for the elastic scattering of protons by Mg^{24} has been measured by Mooring, Koester, Goldberg, Saxon, and Kaufmann in the range of bombarding energies between 0.4 Mev and 3.95 Mev. In the present work, the energy dependence of this cross section is interpreted in terms of the combination of Coulomb and nuclear potential scattering with resonant scattering. This resonant scattering arises from the excitation of energy levels of the compound nucleus Al^{25}. The general trend of the observed cross section between 0.4 Mev and 3.4 Mev, including the three broadest resonances, is well fitted theoretically.

A method is developed to calculate the effects of imperfect energy resolution on the shapes of resonances, and the results are used to rule out certain assignments.

The excited states corresponding to the three broadest resonances have been classified as follows: 3.11 Mev, $P_{3/2}$; 3.88 Mev, $P_{1/2}$; 5.34 Mev, $P_{3/2}$. These energies are the dissociation energy, which is 2.32 Mev, plus the resonant energy in the center-of-mass system. A twofold ambiguity remains in the angular momentum values assigned to the narrow resonances because the experimental resolution was not sufficient to determine their true maximum cross sections. The assignments are as follows: 3.75 Mev, F; 3.91 Mev, D; 4.25 Mev, D; 4.63 Mev, D; 5.83 Mev, D. The last assignment is somewhat doubtful because the phase shifts due to higher, unobserved resonances are not known.

The odd parity levels have reduced widths between 10 percent and 30 percent of the value corresponding to single particle excitation, while the even parity levels have reduced widths only a few tenths of one percent of this value. An explanation of the level structure is offered in terms of a nuclear shell model. The spin-orbit splitting of the 3.11 Mev and 3.88 Mev P states is small compared with doublet splitting observed in closed-shell plus-one nuclei.

I. INTRODUCTION

A PHASE shift analysis of the elastic scattering of protons by a light, spinless nucleus yields the energy, angular momentum, and relative parity quantum numbers of the excited states formed in the compound nucleus. By analyzing the energy dependence of the differential cross section for the elastic scattering of protons by O^{16}, Laubenstein and Laubenstein[1] classified the excited states observed in F^{17}; and Jackson and Galonsky[2] similarly classified levels in N^{13}. The considerations which permit this type of identification of the excited states observed as scattering resonances can be stated briefly. Since the spin of the target nucleus is zero, the angular momentum value j of a state formed in the compound nucleus is given by the relation,

$$j=l\pm 1/2,$$

where l is the orbital angular momentum value of the incident proton and 1/2 is its spin value. In addition the parity P of this state is related to the parity p of the ground state of the target nucleus by the expression,

$$P=(-1)^l p.$$

Only one value of l satisfies both equations; hence a unique combination of spin and orbital angular momentum of the incident proton is specified. Because the resonant scattering interferes with Coulomb and nuclear potential scattering, the qualitative shape of a resonance depends strongly upon the particular values of j and l; thus the angular momentum and parity of the level are determined.

An important consideration in the choice of a target nucleus for these experiments is that the binding energy of the added proton be low. When this requirement is met, a study of the low-lying excited states of the compound nucleus is permitted, and the spectrum is relatively simple. The binding energy of an additional proton to Mg^{24} is only 2.32 Mev,[3] and the angular momentum of the ground state of Mg^{24} is zero.[4] Using the separated Mg^{24} isotope, Mooring, Koester, Goldberg, Saxon, and Kaufmann[5] measured the differential scattering cross section in the region of proton bombarding energies between 0.4 Mev and 3.95 Mev. The present work concerns the interpretation of their results—the classification of levels observed in the compound nucleus Al^{25} and a brief consideration of the theoretical implications of this level structure, especially in connection with the nuclear shell model proposed by Mayer.[6]

The expression used for the differential scattering cross section is presented and discussed in references 1 and 2. The terminology of these papers is followed here, and the same method of analysis is employed.

II. ANALYSIS OF YIELD CURVE

A. The 0.825-Mev Resonance

Figure 1 shows the yield curve obtained by Mooring *et al.*[5] At energies below 0.8 Mev, this curve is well fitted by Rutherford scattering, and thus the absolute

* Supported by the Wisconsin Alumni Research Foundation and the AEC.
† AEC Predoctoral Fellow. Now at University of Illinois, Urbana, Illinois.
[1] R. A. Laubenstein and M. J. W. Laubenstein, Phys. Rev. 84, 18 (1951).
[2] H. L. Jackson and A. I. Galonsky, Phys. Rev. 84, 401 (1951).
[3] Computed from mass values listed in H. A. Bethe, *Elementary Nuclear Theory* (John Wiley and Sons, Inc., New York, 1947).
[4] J. E. Mack, Revs. Modern Phys. 22, 64 (1950).
[5] Mooring, Koester, Goldberg, Saxon, and Kaufmann, Phys. Rev. 84, 703 (1951).
[6] M. G. Mayer, Phys. Rev. 78, 16 (1950).

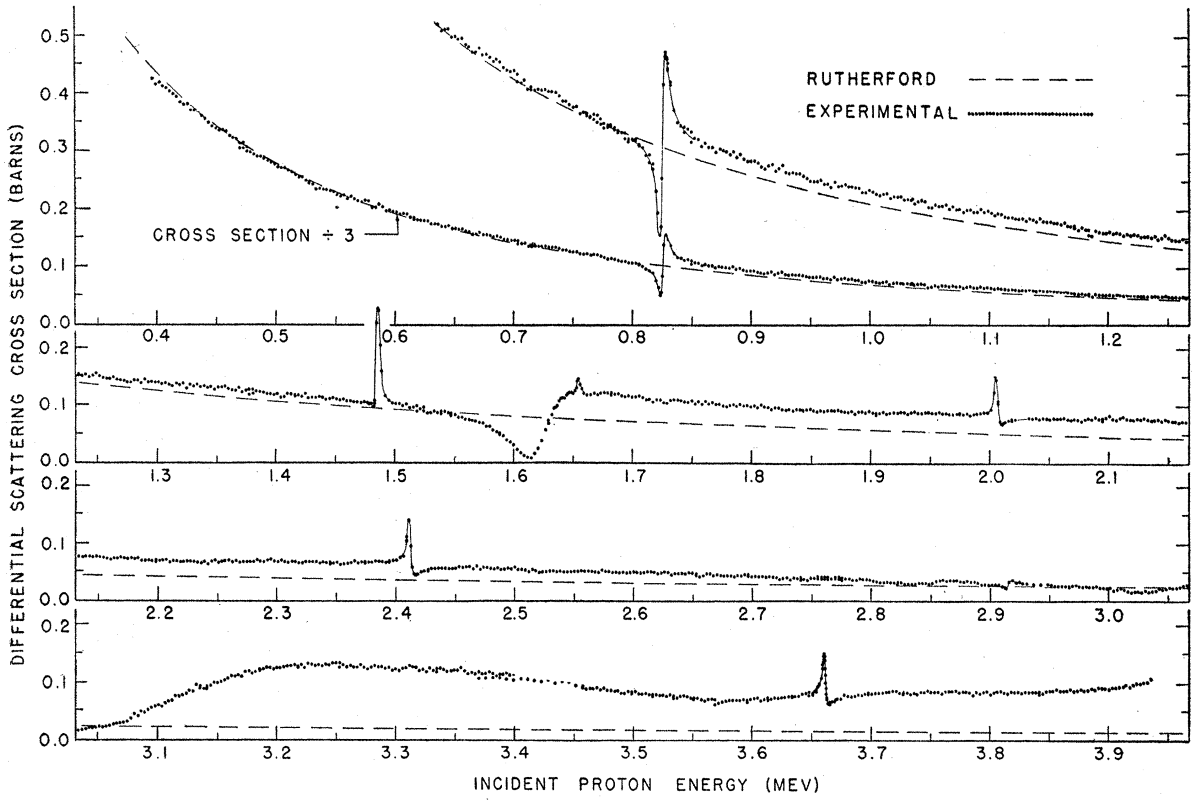

FIG. 1. Differential cross section for the elastic scattering of protons by Mg^{24} at a laboratory angle of 164°±5° (in barns per steradian). From the work of Mooring *et al.* [Phys. Rev. **84**, 703 (1951)].

cross section is determined. The resonance at 0.825 Mev provides a good starting point for the analysis because the nuclear potential phase shifts are all negligible, and in first approximation the scattering formula (see references 1 and 2) reduces to the Rutherford term plus a resonance term. All but two possible assignments of angular momentum and parity can immediately be ruled out on grounds of qualitative shape. Wigner's sum rule on reduced widths[7] is used throughout this analysis to limit the number of l values considered for each resonance according to its observed width. For this first resonance, values of l greater than two need not be considered.

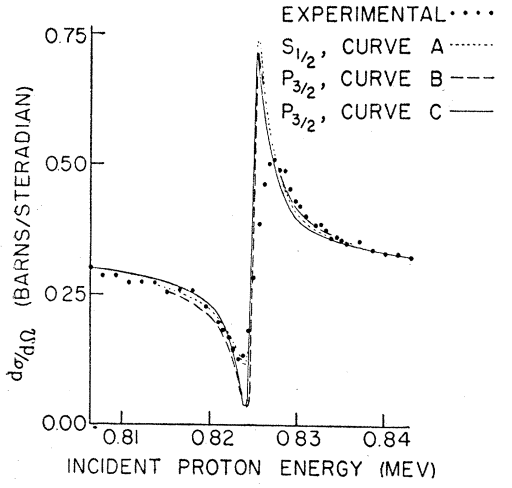

FIG. 2. Theoretical fits of the 0.825-Mev resonance: curve A, approximate calculation for $S_{1/2}$ resonance, in which the incoherent term is neglected and only the resonant phase shift is allowed to vary with energy; curve B, similar approximate calculation for $P_{3/2}$ resonance; curve C, calculation for $P_{3/2}$ resonance without any approximations.

The shape of a $P_{1/2}$ resonance at this energy is qualitatively similar to that of the resonance near 1.6 Mev, with a dip but only a very small maximum, unlike the observed cross section; hence the $P_{1/2}$ assignment is ruled out. The $D_{3/2}$, $D_{5/2}$, $F_{5/2}$, and $F_{7/2}$ assignments are all ruled out because they predict the maximum before the minimum cross section as the energy increases.

Curves A and B of Fig. 2 show, respectively, the approximate calculations for $S_{1/2}$ and $P_{3/2}$ resonances, in which the incoherent term is neglected and only the resonant phase shift is allowed to vary with energy. This approximation is good for an S resonance because the incoherent term is zero. The $P_{3/2}$ assignment is favored here because the averaging effect of imperfect energy resolution in the experiment tends to increase the minimum cross section as well as to decrease the maximum. Better approximations support the con-

[7] E. P. Wigner and L. Eisenbud, Phys. Rev. **72**, 29 (1947); T. Teichmann, Ph.D. Thesis, Princeton University (1949).

TABLE I. Energy levels of Al^{25}, interaction radius: $a_s = 5.05 \times 10^{-13}$ cm.

Bombarding energy in lab system	Resonant energy in center-of-mass system	Resonant energy relative to ground state	Characteristic energy in center-of-mass system	Observed resonance width	Reduced width	Ratio of γ^2 to $\hbar^2/\mu a_s$	Classification
E(Mev)	E_r(Mev)	E_r(Mev)	E_λ(Mev)	Γ(kev)	γ^2(Mev cm)	Percent	
0.825	0.792	3.11	0.405	1.5	2.2×10^{-13}	27.	$P_{3/2}$
1.49	1.43	3.75	1.26	0.3	2.7×10^{-13}	33.	F
1.62	1.56	3.88	1.38	36.	1.7×10^{-13}	21.	$P_{1/2}$
1.66	1.59	3.91	1.59	0.1	$2. \times10^{-15}$	0.2	D
2.01	1.93	4.25	1.93	0.15	$2. \times10^{-15}$	0.2	D
2.40	2.31	4.63	2.31	0.3	$2. \times10^{-15}$	0.2	D
3.14	3.02	5.34	3.03	200.	1.0×10^{-13}	12.	$P_{3/2}$
3.66	3.52	5.83	...	...	...	...	D?

clusion that the 0.825 Mev resonance is a $P_{3/2}$ resonance. Curve C of Fig. 2 shows the fit to the observed cross section that is obtained after the incoherent term, effects of higher resonances, and variation of all the quantities with energy are taken into account. Observation of the scattering at 90° would distinguish conclusively between the $S_{1/2}$ and $P_{3/2}$ possibilities because a P resonance would have no minimum.[1]

The resonant energy is defined herein as the energy, E, in the center-of-mass system, at which the resonance denominator $E_\lambda+\Delta_\lambda-E$ is zero. The characteristic energy E_λ is constant, but the level shift Δ_λ varies with the energy. The value of the observed resonance width Γ is given by the expression

$$\tfrac{1}{2}\Gamma = k\gamma^2/A_l^2,$$

evaluated at the resonant energy; k is the wave number of the incident proton, $1/A_l^2$ is the barrier penetrability, and γ^2 is the reduced width of the level. According to this terminology, the energies and widths of the various levels are given in Table I.

B. The 1.6-Mev Resonance

Because the observed resonance width increases with the wave number and barrier penetrability of the incident proton, the resonant phase shift due to the 0.825-Mev resonance never exceeds 176° in the energy range considered. Similarly, the broad resonances at 1.6 Mev and 3.1 Mev contribute to the phase shifts over most of this energy range. In the analysis of the yield curve, therefore, one must first identify these broad resonances and then piece them together to fit the general trend of the curve. The narrow resonances can then be superimposed without disturbing this fit.

The next resonance to be analyzed is the one that consists of the broad minimum near 1.6 Mev and the broad, flat maximum at higher energies. The small peak near 1.65 Mev is a separate resonance, so narrow that its influence is limited to a region of a few kilovolts; hence it is omitted in the first approximation. The only resonance assignment that does not predict a high maximum cross section at this energy is $P_{1/2}$. The qualitative agreement of the approximate calculation for a $P_{1/2}$ resonance with the experimental results is shown in Fig. 3.

The value of the incoherent term at the minimum cross section is 0.01 barn, which is just the value needed to account for the experimental cross section. Curve B of Fig. 3 shows the result of including the incoherent term and of letting the proton wavelength, the resonant energy, the observed resonance width, and the Rutherford and nuclear potential vectors vary with energy in the calculation. This calculation does not include the effects of other resonances.

C. The Cross Section above 2.8 Mev

The cross section between 2.8 Mev and 3.4 Mev can be interpreted in terms of a single broad resonance, although the shallow minimum near 3.6 Mev suggests another broad resonance at higher energies. The assignment for the resonance between 2.8 Mev and 3.4 Mev can be restricted to $S_{1/2}$ or $P_{3/2}$ on the basis of qualitative shape. The maximum cross section predicted by a $P_{1/2}$ resonance is about half the observed maximum, and the maximum of any of the D or F resonances is much too large.

Figure 4 shows the results of the approximate calculations for $P_{3/2}$ and $S_{1/2}$ resonances. The maximum cross section is too great in either case, although it is worse for the $S_{1/2}$ resonance. More accurate calculations do not improve these fits.

As Jackson and Galonsky[2] state, a value for the interaction radius must be chosen at the beginning of

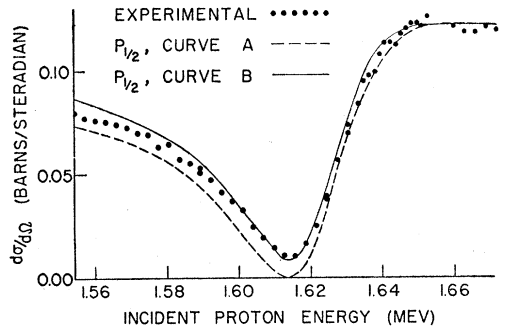

FIG. 3. Theoretical fits of the 1.6-Mev resonance: curve A, approximate calculation for $P_{1/2}$ resonance; curve B, calculation for $P_{1/2}$ resonance without approximations, except that effects of other resonances are omitted.

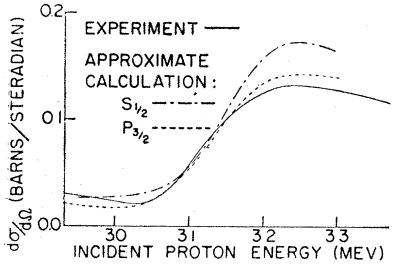

FIG. 4. Approximate calculations for $S_{1/2}$ and $P_{3/2}$ resonances near 3.1 Mev for the interaction radius value 5.83×10^{-13} cm.

the analysis. The first value chosen in this work was

$$a_s=1.5\times10^{-13}(A^{1/3}+1^{1/3})=5.83\times10^{-13}\text{ cm},$$

where A is the mass number of Mg^{24}. If all existing resonances are properly taken into account, a fit to the cross section can, in principle, be obtained with any value of the interaction radius in the approximate range from $1.5\times10^{-13}A^{1/3}$ cm to $1.5\times10^{-13}(A^{1/3}+1)$ cm. This statement is verified for the fits of the lower resonances in this experiment.

In the analysis of the cross section between 2.8 Mev and 3.4 Mev, however, a little experimenting shows that the $P_{3/2}$ resonance can be brought into reasonable agreement with observation by changing the value of the interaction radius to 5.05×10^{-13} cm, which lies midway between the above limits. Figure 5(a) shows the result. This calculation includes all the terms of the formula and allows all of the quantities to vary with energy. Phase shifts due to lower resonances are also included. The sharp resonance at 3.65 Mev is omitted because it is not expected to influence the rest of the curve.

The fit of the $S_{1/2}$ resonance is not good for any reasonable value of the interaction radius. The result of the exact calculation for an $S_{1/2}$ resonance with the new value of the interaction radius is shown in Fig. 5(b).

For simplicity, the interaction radius was assumed to be constant for all energies and for all l values of the incident proton. After the value was changed to 5.05×10^{-13} cm, the lower resonances were recalculated. The only changes involved were in the values of the characteristic energies and reduced widths. The classifications and the fits were not affected.

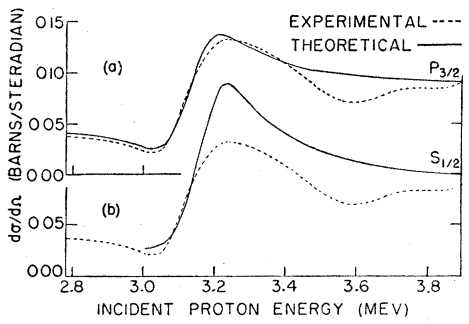

FIG. 5. (a) Calculation for a $P_{3/2}$ resonance near 3.1 Mev (without approximations) if the interaction radius has the value 5.05×10^{-13} cm. (b) Calculation for an $S_{1/2}$ resonance (without approximations) for this value of the interaction radius.

As Fig. 5(a) shows, the observed minimum in the cross section near 3.6 Mev is not reproduced by the calculation for a $P_{3/2}$ resonance alone. It is also highly unlikely that this broad dip is associated with the narrow resonance at 3.65 Mev. Since the introduction of a resonance broad enough to produce this dip destroys the existing fit below 3.4 Mev, the cross section must be refitted in the whole interval between 2.8 and 3.9 Mev. Attempts were made to fit the cross section in this interval with various combinations of two resonances. No combinations of three resonances were considered.

Pairs of resonances of the same angular momentum and parity, such as $S_{1/2}-S_{1/2}$, can immediately be ruled out on the same grounds as for the case of a single resonance of the same angular momentum and parity. The expression for the resonant phase shift is

$$\beta=\tan^{-1}\left[\frac{\frac{1}{2}\Gamma_1}{E_1+\Delta_1-E}+\frac{\frac{1}{2}\Gamma_2}{E_2+\Delta_2-E}\right],$$

where the subscripts 1 and 2 refer to the two resonances. Thus, the vector diagram still involves only one circle, and the cross section must pass through essentially the same maximum and minimum as if there were only a single resonance. The end point of the resonance vector traverses the circle more rapidly with energy than in the case of a single resonance, and goes twice around the circle. A pair of $P_{3/2}$ resonances is the only combination of this type that might appear possible, and the second minimum cross section predicted by this combination is much too small.

A slight modification of the vector diagram permits a study of the cross section predicted by a pair of resonances with a minimum of numerical calculation. One of the resonance vectors can be added to the end of the Rutherford vector as usual, while the other is added to the beginning of the potential vectors. The locus of starting points of this second resonance vector is the usual circle reflected in the point $\delta=0$, and the beginning of the vector traverses this circle in a counterclockwise direction as the phase shift δ increases. Figure 6 shows a diagram of this type in which a $P_{1/2}$ resonance vector is added to the beginning of the potential vectors and an $S_{1/2}$ resonance vector to the end of the Rutherford vector. In the first approximation, the cross section is proportional to the square of the distance $|A|$ measured between points on the two circles. Since the values of $|A|$ corresponding to the cross sections at the first minimum (3.0 Mev), the maximum (3.2 Mev), and the second minimum (3.6 Mev) are about 0.5, 1.4, and 1.0 unit, respectively (see scale at bottom of Fig. 6), inspection of this diagram rules out the $S_{1/2}-P_{1/2}$ combination.

All other pairs of resonances are ruled out in a similar manner except $P_{3/2}-S_{1/2}$ and $P_{3/2}-P_{1/2}$. The

best fits obtained with these combinations, by means of the complete formula, are shown in Fig. 7.

The conclusion drawn from these results is that the cross section between 2.8 and 3.4 Mev can be interpreted most simply in terms of the $P_{3/2}$ resonance shown in Fig. 5(a), but that the cross section above 3.4 Mev can probably not be explained without additional data. Extension of the elastic scattering data to higher energies and other angles, and further study of the inelastic scattering cross sections would probably be helpful.

D. General Trend of the Cross Section

The three broad resonances discussed above must now be joined together to fit the general trend of the cross section over the entire energy range of observation. In the scattering formula, the phase shift $\delta_{l\pm}$ is always given by the expression

$$\delta_{l\pm}=\beta_{l\pm}-\phi_l,$$

where ϕ_l is the potential phase shift and $\beta_{l\pm}$ is the resonant phase shift. In this calculation, the $P_{3/2}$ resonant phase shift is

$$\beta_1{}^+=\tan^{-1}\left[\frac{\frac{1}{2}\Gamma_1}{E_1+\Delta_1-E}+\frac{\frac{1}{2}\Gamma_2}{E_2+\Delta_2-E}\right],$$

where the subscripts 1 and 2 refer to the $P_{3/2}$ resonances near 0.825 Mev and 3.1 Mev, respectively. If more $P_{3/2}$ resonances were known, they would be included in this sum. Similarly,

$$\beta_1{}^-=\tan^{-1}[\tfrac{1}{2}\Gamma_3/(E_3+\Delta_3-E)],$$

where the subscript 3 refers to the $P_{1/2}$ resonance near 1.6 Mev, the only one known. All other resonant phase shifts are neglected.

Computed values of the cross section are shown as solid circles in Fig. 8, and the solid curve is traced through the experimental points of Fig. 1. Calculations show that none of the narrow resonances contribute phase shifts that could appreciably change this fit between resonances. The general excellence of this fit below 3.4 Mev is taken as evidence that the interpretation presented thus far is correct and that it is safe to proceed to the identification of the narrow resonances.

E. Effects of Imperfect Energy Resolution

The observed half widths of the narrow peaks in the cross section near 1.5, 1.65, 2.0, 2.4, and 3.65 Mev (see Fig. 6 of reference 5) are all approximately equal to the energy spread of the proton beam combined with that introduced by energy loss in the target. The actual peaks may be much narrower and higher than the observed peaks. In each of these cases, the only theoretical resonances possessing the right qualitative shape predict a maximum cross section much higher than that observed. To discover how narrow the resonance must be in order that its maximum be degraded by the effects

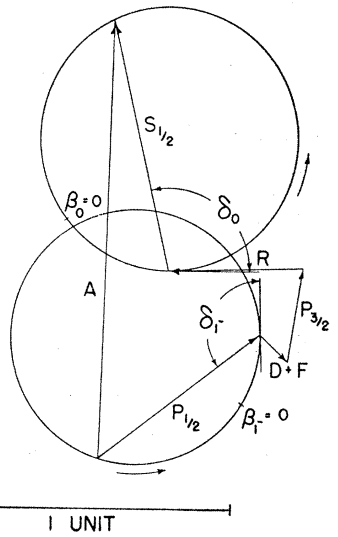

FIG. 6. Vector diagram for a combination of an $S_{1/2}$ and a $P_{1/2}$ resonance above 3 Mev. The beginning of the $P_{1/2}$ vector starts at the point marked $\beta_1{}^-=0$ and traverses the circle in a counterclockwise direction as energy increases. This point does not coincide with the point $\delta_1{}^-=0$ because the potential phase shift is about 9°. Similarly, the end of the $S_{1/2}$ vector starts at the point marked $\beta_0=0$ and traverses its circle in a counterclockwise direction. In first approximation, the cross section is proportional to the square of the length of the resultant A. The scale gives the length corresponding to unit amplitude (dimensionless).

of imperfect energy resolution to the value observed, a method is developed to compute the observed cross section from the theoretical curve.[8] This method cannot be used to prove that a given assignment is correct, but it can be used in conjunction with the sum rule on reduced widths[7] to rule out certain assignments.

When the cross section is measured at an energy E, which is determined by the voltage of the electrostatic generator, the number of incident protons with energies between E' and $E'+dE'$ is $Qg(E-E')dE'$, where Q is the total number of protons incident, and $g(E-E')$ is the energy distribution of protons in the beam. This function is triangular[9] in shape and is normalized. After a proton of energy E has penetrated a distance x into the target, its energy has decreased to the value $E-ax$, where a is the stopping power of the target material. The energy distribution of protons at the depth x in the

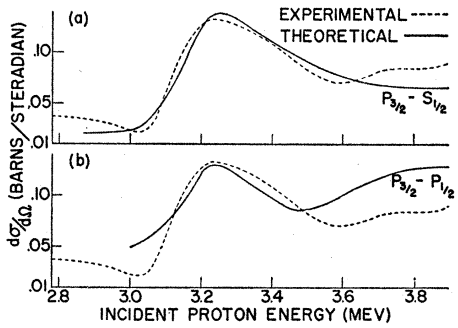

FIG. 7. (a) Calculation for a combination of a $P_{3/2}$ and an $S_{1/2}$ resonance above 3 Mev (without approximations). (b) Calculation for a combination of a $P_{3/2}$ and a $P_{1/2}$ resonance above 3 Mev (without approximations).

[8] J. L. Powell has developed a similar method to apply to reaction cross sections (symmetric resonance peaks) (private communication).

[9] Herb, Snowden, and Sala, Phys. Rev. **75**, 246 (1949).

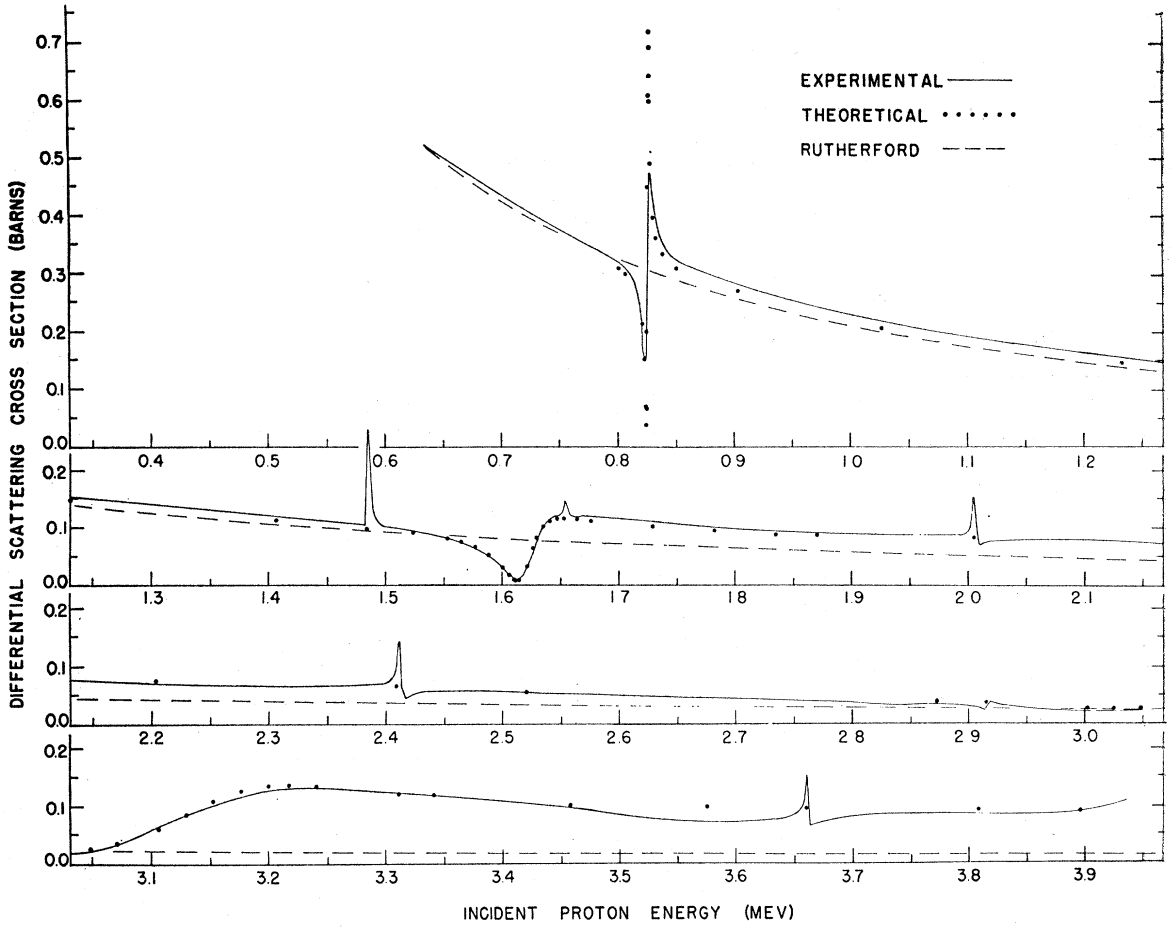

FIG. 8. Theoretical cross sections (solid circles) compared with the experimental curve (traced through the points of Fig. 1). Effects of narrow resonances were omitted in these calculations. The interaction radius value 5.05×10^{-13} cm is used throughout.

target is thus $g(E-v-E')$, where $v=ax$. The effect of thermal motion in the target is neglected, although it contributes an energy spread of the order of 100 ev.

The measured differential cross section at the nominal energy E and angle θ is

$$\sigma_0(E,\theta)=\frac{1}{at}\int_0^{at}dv\int_{E-v-\delta}^{E-v+\delta}g(E-v-E')\sigma(E',\theta)dE',$$

where at is the target thickness in energy units, δ is the maximum deviation of protons in the beam from the energy E, and $\sigma(E',\theta)$ is the theoretical cross section at the energy E'. Since this cross section is not a simple function of energy, numerical or graphical integration over energy is necessary. The order of integration is therefore changed. The integration over target thickness is elementary and results in an expression of the form,

$$\sigma_0(E,\theta)=\frac{1}{at}\int_{E-\delta-at}^{E+\delta}\sigma(E',\theta)F(E'-E)dE',$$

where the function $F(E'-E)$ (see Fig. 9) gives the distribution of energies available for collisions in the target. The integrand for any value of E' is obtained by reading the corresponding values of $F(E'-E)$ and $\sigma(E',\theta)$ from their graphs and multiplying them together. The result of the integration is the cross section $\sigma_0(E,\theta)$ that would be observed at the nominal energy E if the proposed cross section curve were correct. By repeating the integration for a series of energies E similar to those used in the experiment, one obtains a cross section curve to be compared with the one actually observed. If this comparison is good, the proposed cross section curve is plausible, although it may not be unique. The result of this treatment is that the qualitative shape of a resonance is preserved even though the energy distribution function is several times wider than the resonance, but that peaks are spread out and flattened. It follows from the normalization of the function $F(E'-E)$ that the area between the energy axis and the cross section curve of a resonance is conserved.

F. The 1.485-Mev Resonance

The F and G resonances are the only ones that predict the qualitative shape of the peak in the cross section observed at this energy. The G resonances are

ruled out because, even if the width be chosen equal to the upper limit, the area under the calculated curve is much less than that under the experimental curve. Figure 10 shows an $F_{5/2}$ resonance compared with the experimental data. The area under the theoretical curve was made equal to that under the experimental curve by setting the width Γ equal to 300 ev, which corresponds to a reduced width of about a third or fourth of the upper limit. In this and all the other calculations for the narrow resonances, the incoherent term is included, but only the resonant phase shift is allowed to vary with energy.

In view of the above arguments, there appears to be good evidence that this resonance has odd parity relative to Mg^{24}, and that its angular momentum value is either 5/2 or 7/2. The only distinction between these two values would be in the height of the peak.

G. The 1.655-Mev Resonance

This resonance is extremely narrow, and its maximum appears at a lower energy than its minimum. On the basis of this qualitative shape, circle diagrams immediately rule out all possibilities except D and H resonances. The upper limit computed for the observed width of an H resonance is 10 ev. It seemed doubtful that a resonance this narrow could be observed at all, and for this reason the study of resolution effects described in Sec. E was undertaken.

Figure 11(a) shows that an $H_{11/2}$ resonance has a shape qualitatively similar to the observed shape, except that the maximum is 3 barns instead of 0.19 barn. The observed cross section to be expected on the basis of the instrumental resolution is calculated point by point, with the result shown in Fig. 11(b). It would be necessary to double or triple the width in order to make this curve coincide with the experimental curve, and this seems to be a sufficient argument to rule out an H resonance.

The same procedure was carried out for a $D_{5/2}$ resonance with a width of 100 ev. The theoretical cross section and the observed cross section to be expected are shown in Fig. 12. The result indicates that the resonant energy and width chosen were both too large, but with small adjustments the curve might be brought into agreement with experiment. The reduced width of this resonance is only a few tenths of one percent of the upper limit. This resonance appears to have even parity and either 3/2 or 5/2 units of angular momentum.

H. The Resonances Near 2.01 Mev and 2.41 Mev

These resonances are similar to the one just considered in that each is narrow and each has a maximum at lower energies than the minimum. At these energies, however, the H circle is reoriented so that only the D resonances have the proper qualitative shape. Figure 13 compares $D_{5/2}$ and $D_{3/2}$ resonances with the cross section near 2.01 Mev, and Fig. 14 shows a $D_{3/2}$ resonance near 2.41 Mev. In each case, the reduced width is only a few tenths of one percent of the upper limit.

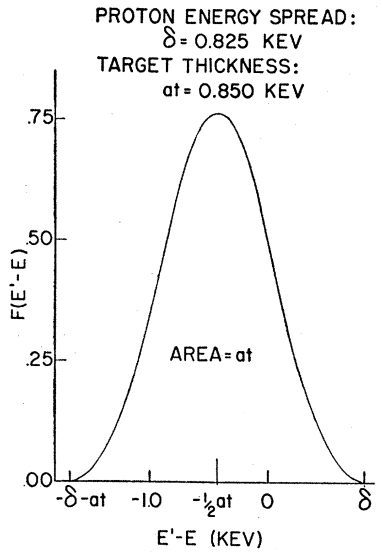

FIG. 9. The distribution of energies available for collisions in the target, for a bombarding energy, E, of 1.655 Mev. This calculation neglects the effects of thermal motion.

At 2.41 Mev a peak in the inelastic scattering was observed.[5] The fact that the elastic scattering width is less than the total width may partially explain why the maximum cross section observed is less than that predicted by the formula. These two levels are assigned even parity and angular momentum quantum numbers of either 3/2 or 5/2.

I. The Cross Section near 2.91 Mev

The small variation in the cross section near 2.91 Mev was studied only with the survey target,[5] and the shape is not well determined. No definite assignment of quantum numbers can be made, but a brief investigation was carried out to determine the possibilities. Cal-

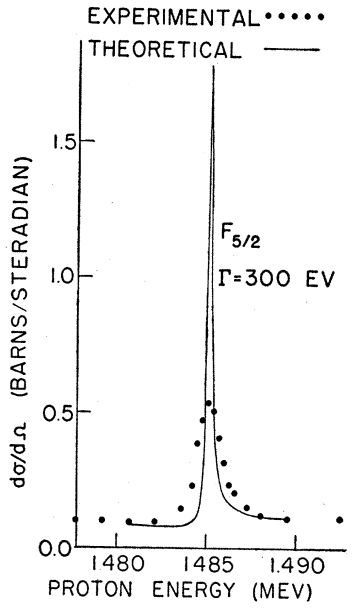

FIG. 10. Comparison of an $F_{5/2}$ resonance with the observed resonance at 1.485 Mev. The width is chosen to make the areas under the two curves equal.

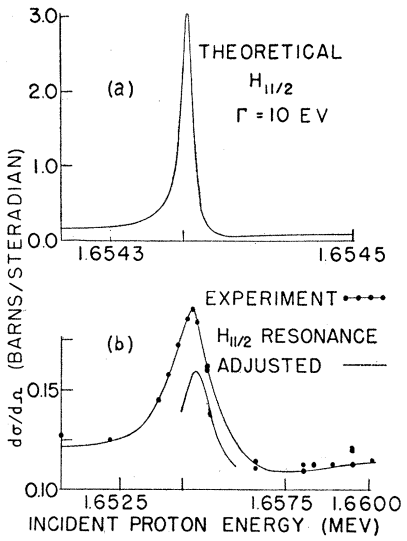

FIG. 11. (a) Theoretical shape of an $H_{11/2}$ resonance near 1.655 Mev. (b) Comparison of experimental data with this $H_{11/2}$ resonance adjusted for effects of finite energy resolution. Note the difference in scales of graphs. Energy scales coincide at the marks under the peaks.

culations show large fluctuations in the cross section associated with any resonance up to $l=6$. Circle diagrams indicate that an S resonance has the best qualitative shape, but the maximum would be about 0.13 barn and the reduced width extremely small. That this resonance can be attributed to an impurity in the target is rather unlikely because it exhibits a minimum, and impurities scatter incoherently.

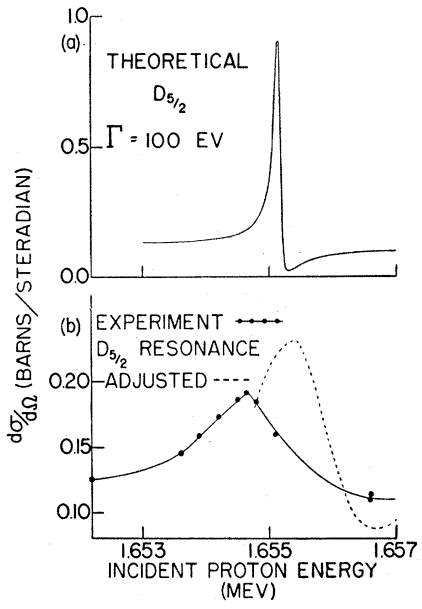

FIG. 12. (a) Theoretical shape of a $D_{5/2}$ resonance at 1.655 Mev; (b) Comparison of experimental data with this $D_{5/2}$ resonance adjusted for effects of finite resolution, showing that the resonant energy and width chosen were too large. Note difference in scale of ordinates.

J. The 3.65-Mev Resonance

This resonance also was studied only with the survey target, but its qualitative shape is clearly similar to those at 2.01 and 2.41 Mev. The principal difficulty in identifying this resonance is that the other phase shifts in the vicinity are not well understood. The background fit (Fig. 8) deviates markedly from experiment here. It is likely, however, that the phase shifts which form the potential background are not grossly in error, and that future changes will be small. Circle diagrams indicate that very large changes in the potential phase shifts would be necessary to make anything but a D resonance look reasonable, if resonances up to $l=6$ are considered.

The S wave phase shift at this energy is about $-29°$. If it were zero or a few degrees positive, a D resonance would fit the data very well. The background cross section under this condition would also agree with observation. Unfortunately, however, it seems impossible to choose parameters for an $S_{1/2}$ resonance such that the cross section agrees with experiment over the entire interval of observation. Under the circumstances, it appears that a definite classification of the 3.65 Mev resonance is not justified.

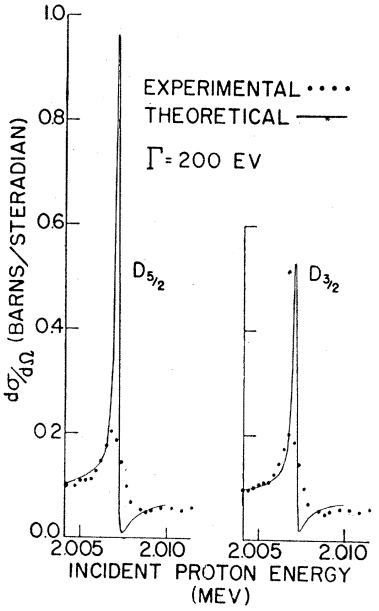

FIG. 13. Comparison of $D_{5/2}$ and $D_{3/2}$ resonances with experimental cross sections near 2.01 Mev.

K. Summary of Analysis

The interpretation of the three broad resonances near 0.825, 1.6, and 3.1 Mev is simple and unambiguous. They all have odd parity relative to Mg^{24}, and they have reduced widths of the order of 10–30 percent of the single particle limit $\hbar^2/\mu a_s$, where μ is the reduced mass and a_s is the interaction radius.[10] The analysis of the 1.49-Mev resonance leaves a twofold ambiguity in the angular momentum value, but the evidence for odd

[10] R. K. Adair, Phys. Rev. 82, 750 (1951).

parity is fairly strong. The reduced width of this resonance seems to be of the same order of magnitude as those of the first three mentioned.

All of the other resonances observed seem to have very small reduced widths. With the exception of the one near 2.91 Mev, about which little is known, they all appear to have even parity and 3/2 or 5/2 units of angular momentum. The high energy cross section seems to indicate a combination of two or more broad resonances above 3 Mev, but the yield curve could not be fitted simultaneously at all energies with any combination of two resonances in this region.

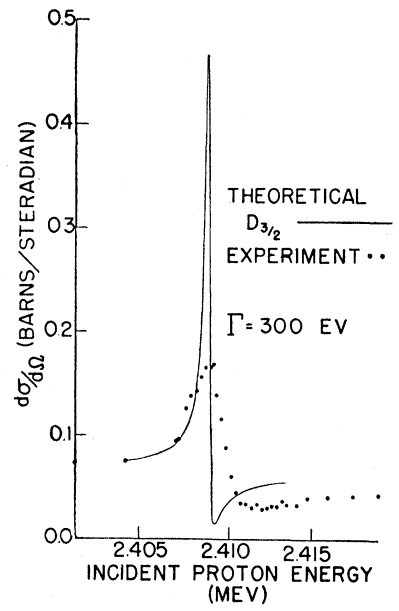

FIG. 14. Comparison of a $D_{3/2}$ resonance with experimental cross sections near 2.41 Mev.

III. CONCLUSION

A. Energy Level Diagram and Mirror Nucleus

Figure 15 shows the energy levels of the mirror nuclei Mg^{25} and Al^{25} placed so that the ground states coincide. The excitation energy of each level plotted in Al^{25} is the dissociation energy, which is 2.32 Mev, plus the resonant energy E_r, in the center-of-mass system. This energy is used in preference to the characteristic energy E_λ, because although E_λ is associated with the internal wave functions of the compound nucleus, its value depends on the choice of interaction radius. The two lowest excited states shown in Al^{25} were observed by Grotdal *et al.*[11] but not by Mooring *et al.*[5]

The Mg^{25} levels are taken from the results of Schelberg, Sampson, and Cochran.[12] These are all bound levels in that their energies are less than the dissociation energy of a proton or neutron, and none of them is classified. For the present, therefore, the comparison shows only that the level densities are about the same in the two nuclei.

B. Characteristic Energies, Reduced Widths, and Interaction Radii

In principle, the exact value of the interaction radius is not important to the analysis. The values of the characteristic energies and reduced widths of resonances do, however, depend on the value chosen for the interaction radius. Table II compares the values of these parameters of the broad resonances near 0.825 Mev and 1.6 Mev for two different values of the radius. Although these results should not be generalized, they are in qualitative agreement with theoretical predictions by Wigner and Eisenbud and by Teichmann.[7]

C. Comparison with the Shell Model of the Nucleus

According to the shell model proposed by Mayer,[6] the levels that are filled by protons (and by neutrons) in Mg^{24} are given by the expression

$$(1s_{1/2})^2(1p_{3/2})^4(1p_{1/2})^2(1d_{5/2})^4,$$

where the superscript indicates the number of protons (or of neutrons) occupying the state. Since only four of the six available $d_{5/2}$ states are filled, the additional proton is assumed to occupy a $d_{5/2}$ state for the ground state of Al^{25}. This assumption is verified experimentally[4] for the additional neutron in Mg^{25}.

If the single particle picture were valid, the sequence of excited states in Al^{25} should be the same as that following $1d_{5/2}$ in Table II of reference 6, with the provision that spin-orbit splitting might cause pairs of levels like $2p_{3/2}$ and $1f_{5/2}$ to cross. The degree of validity of the

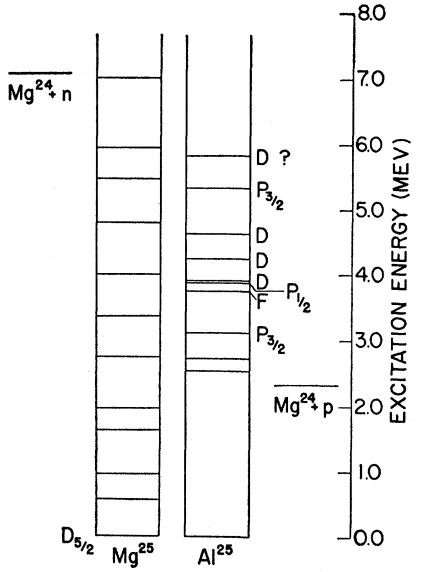

FIG. 15. Energy level diagrams of Mg^{25} (from the data of Schelberg, Sampson, and Cochran [Phys. Rev. **80**, 574 (1950)]) and Al^{25}. Excitation energies in Al^{25} are the dissociation energy (2.32 Mev) plus the resonant energy in the center-of-mass system. The two lowest excited states in Al^{25} were observed by Grotdal *et al.* (reference 11).

[11] Grotdal, Lönsjö, Tangen, and Bergström, Phys. Rev. **77**, 296 (1950).
[12] Schelberg, Sampson, and Cochran, Phys. Rev. **80**, 574 (1950).

TABLE II. Reduced width and characteristic energy for two values of the interaction radius a_s: $a_s=5.83\times10^{-13}$ cm., $a_s=5.05\times10^{-13}$ cm.

Resonant energy center-of-mass system	Observed resonance width	$a_s=5.83\times10^{-13}$cm		$a_s=5.05\times10^{-13}$cm	
		Reduced width	Characteristic energy	Reduced width	Characteristic energy
E(Mev)	Γ(kev)	γ^2(Mev cm)	E_λ(Mev)	γ^2(Mev cm)	E_λ(Mev)
0.792	1.5	1.2×10^{-13}	0.61	2.2×10^{-13}	0.41
1.557	36.	1.0×10^{-13}	1.47	1.7×10^{-13}	1.38

single particle approximation for a certain state may be estimated by the ratio of the value of its reduced width to the value of $\hbar^2/\mu a$.[10] Four of the levels classified in Al^{25} have reduced widths greater than ten percent of the single particle value. These are the $P_{3/2}$ level at 3.11 Mev, the F level at 3.75 Mev, the $P_{1/2}$ level at 3.88 Mev, and the $P_{3/2}$ level at 5.34 Mev. These energies are measured from the ground state as in Fig. 15. If the angular momentum value of the F level is 5/2, the first three of these levels fit into the predicted sequence. The $1d_{3/2}$, $2s_{1/2}$, and $1f_{7/2}$ levels might then lie in the region below the classified levels.

None of the other resonances observed is considered to represent a single particle level because the values of their reduced widths are only a few tenths of one percent of the limit. The abundance of narrow levels of even parity is striking and deserves some consideration. If some of the core nucleons are excited in the bombardment of Mg^{24}, the mean life of the state of the compound nucleus is greater than it would be if only the added proton were excited, because time is required for the energy to be concentrated on the emitted proton. By the uncertainty principle, therefore, the width of a level involving multiple particle excitation is smaller than that of a single particle level.

Of the core nucleons, those in the unfilled $1d_{5/2}$ shell should be most easily excited. In the region of excitation above 3.88 Mev, the energy required to excite two or more of these nucleons into the next lowest unoccupied states (e.g., $1d_{3/2}$, $2s_{1/2}$, $\cdots$) might be less than that required to excite a single proton into the $1g_{9/2}$ state. Since these two lowest unoccupied states are of even parity, as are the $1d_{5/2}$ states, one might expect a fairly large number of multiple particle states of even parity.

A subject of current interest is the spin-orbit splitting of nuclear energy levels. In the present experiment, a $P_{3/2}-P_{1/2}$ doublet is observed (the 3.11-Mev and 3.88-Mev levels of Fig. 15). The separation is approximately 0.77 Mev. This splitting is rather small compared with the 5-Mev splitting of the $P_{3/2}-P_{1/2}$ doublets[10] in He^5 and Li^5, and compared with the 4.4-Mev splitting of the $D_{5/2}$ and $D_{3/2}$ levels[1] in F^{17}. Correlation of recent evidence obtained by Bockelman *et al.*[13] with the assignments of Jackson and Galonsky[2] indicates that the $D_{5/2}-D_{3/2}$ splitting in C^{13} and N^{13} is of the order of 3 Mev. The above levels in He^5 and Li^5, however, have very large reduced widths, corresponding to single particle excitation, and the same is true to a lesser extent of the D levels in C^{13}, N^{13}, and F^{17}, while these two P levels in Al^{25} are only approximately "twenty-percent-single-particle" levels. Also, He^5, Li^5, C^{13}, N^{13}, and F^{17} are closed-shell-plus-one nuclei; and the energies of the lowest excited states of the core nuclei, He^4, C^{12}, and O^{16}, are greater than 4 Mev.

The foregoing discussion is rather speculative in nature, but the simplicity of this level structure for a nucleus like Al^{25} is fascinating. Although these suggestions may be incorrect, simplifying assumptions seem to be indicated, and the gradual accumulation of systems of classified excited states of nuclei may result in similarities of structure that will lead to a better picture of the nucleus.

The author wishes to express his gratitude to Professor R. G. Herb for inspiration and guidance. Valuable discussions with Professor H. T. Richards and Dr. R. K. Adair and Dr. F. P. Mooring are also gratefully acknowledged.

[13] Bockelman, Miller, Adair, and Barschall, Phys. Rev. 84, 69 (1951).